International Journal of Innovative Computing, Information and Control
Volume **18**, Number **1**, February **2022**

ICIC International ©2022 ISSN 1349-4198
pp. **253–270**

FUZZY STATE-FEEDBACK CONTROL FOR MPPT OF PHOTOVOLTAIC ENERGY WITH STORAGE SYSTEM

Karima El Hammoumi, Redouane Chaibi and Rachid El Bachtiri

Industrial Technologies and Services Laboratory
Higher School of Technology
Sidi Mohamed Ben Abdellah University
Fez 30000, Morocco
{ karima.elhammoumi; redouane.chaibi; rachid.elbachtiri }@usmba.ac.ma

Received May 2021; revised September 2021

Abstract. *This paper presents maximum power point tracking (MPPT) control for photovoltaic systems with battery storage using the Takagi-Sugeno (T-S) fuzzy model based approach. Under varying meteorological conditions, we consider a DC-DC boost converter to control the output power of a photovoltaic panel array. A T-S reference model is used to generate the optimum trajectory, which must be tracked in order to achieve optimal power point. Controller gains are obtained by solving a set of linear matrix inequalities (LMIs). Furthermore, the proposed method eliminates the oscillation disadvantage near the maximum power point while also reducing tracking time. Finally, the simulation of the photovoltaic system using the proposed control demonstrates the efficacy of the proposed algorithm even in the case of climate change.*
Keywords: Photovoltaic system, Batteries, Boost converter, Maximum power point traking, Takagi-Sugeno fuzzy systems

1. **Introduction.** Currently, the misdeeds of the massive use of fossil fuels for electrical production, the demand for which is continuously growing are well-known greenhouse effect, atmospheric pollution, disturbances and global warming, etc. This awareness, as well as many other economic and political reasons, incites and motivates the scientific community to reflect on the development of renewable energies and their optimal use. Indeed, renewable energies such as photovoltaic (PV) offer many advantages because there is no greenhouse gas emission during electricity production. Sunlight is available everywhere and can be harnessed in the mountains as well as in the cities. However, PV production is variable and strongly depends on climatic conditions (solar irradiation, temperature) which are often unstable [1, 2, 3].

Therefore, due to their intermittent nature, PV systems cannot ensure a continuous supply of energy on their own. In order to make that this energy is both reliable and efficient, it is necessary to overcome two main problems related to the production of photovoltaic energy in an isolated site: the operation difficulty at the optimal point and the storage of the produced energy [4]. Because of their low cost and lengthy autonomy [5], lead-acid batteries are extensively employed to store the energy produced by GPVs on isolated sites, and they provide a pretty good performance/cost ratio.

The use of MPPT (maximum power point tracker) [5] is required to obtain the maximum energy from the PV generator regardless of climatic circumstances. The MPPT is based on hardware and software aspects: DC-DC converter to adapt the load impedance

DOI: 10.24507/ijicic.18.01.253

to the source of the PV generator and an MPPT algorithm (maximum power point tracking) to achieve maximum power at all times [6]. Likewise, an enormous number of MPP tracking algorithms have been developed in the literature. Techniques are very diverse but all fix the operating point of the system by acting on the duty cycle of the DC-DC converters and differ in degree of complexity, in the number of sensors required, in the speed of convergence and cost of monitoring efficiency [7]. Each of these techniques has advantages and disadvantages. The best known are the Perturb and Observe (P&O) methods [8] and the incremental conductance (IC) methods [9]. These approaches have the advantage of being simple to implement, but they are unstable (oscillations around the maximum point). Improved versions of the P&O approach based on adaptive techniques [10, 11] allow for the reduction or cancellation of oscillations around the maximum point, but this adds complexity and does not solve the robustness problem (difficulty of following quick changes in weather conditions) [12]. In order to overcome such difficulties, various strategies have been developed, among which a successful approach is a Takagi-Sugeno (T-S) fuzzy control.

Since 1985, T-S fuzzy systems have been used to control nonlinear systems and solve many analysis and control design problems for these systems. In addition, T-S fuzzy systems play a significant role in the synthesis of fuzzy controllers [13]. T-S fuzzy controllers provide a simple analytical expression of the output generated as a function of the considered inputs, which makes it possible to exploit numerical optimization mechanisms for their synthesis such as least-squares algorithms [14, 15, 16]. This method has been used in several works in order to solve the problem of tracking [17, 18]. Despite all of this development, conservatism remains a problem that requires more research.

Based on the motivation above, we propose an MPPT T-S fuzzy controller of a photovoltaic system with variations of the temperature and the radiations. The designed MPPT controller is developed to a PV system, including a PV module, a DC-DC boost converter and a battery load. Sufficient conditions for the existence of an MPPT fuzzy controller are presented using the quadratic Lyapunov function. Moreover, it is easy to see that the controller parameters can be derived by solving a set of rigorous LMIs, using existing LMI solvers. In comparison to the previous study methods, the MPPT fuzzy controller presented in this paper has a powerful ability to force the PV generator to operate very close to the maximum power trajectory, reducing the required sensors by estimating the output voltage by an adaptation mechanism, and reduces the oscillations around the MPP. The remainder of this paper is organized as follows. The PV system description is presented in Section 2. Section 3 describes the T-S fuzzy modeling and identification. In Section 4, the analysis based on the simulation results is conducted. The conclusion is given in Section 5.

Notations: Through this paper, $sym(M)$ represents $M + M^T$. M^T denotes the transpose of M. The symbol $*$ represents the symmetric term in a block matrix. I denotes the identity matrix with appropriate dimension. $P > 0$ (< 0) means that P is positive (negative) definite matrices.

2. System Description and Modeling.

The photovoltaic system used in this work is shown in Figure 1. It is composed of an $MSX60$ PV module coupled to a DC-DC converter and a battery load, driven by an MPPT assuming the maximum efficiency for the energy transfer.

2.1. Modeling of the PV generator.

As shown in Figure 2, the solar cell is equivalent to a light current source connected in parallel with a diode and a shunt resistor, and all

are coupled to a series resistor [19, 20]. The analytic expression of the current delivered by the PV panel is given by

$$I_{pv} = I_{ph} - I_d - I_{sh} = I_{ph} - I_0 \left[\exp\left(\frac{V_{pv} + R_s I_{pv}}{nV_T}\right) - 1\right] - \left(\frac{V_{pv} + R_s I_{pv}}{R_{sh}}\right) \tag{1}$$

where

$$V_T = \frac{KT}{q}$$

$$I_{ph} = [I_{scr} + K_i(T - T_r)]\left(\frac{G}{1000}\right) \tag{2}$$

where I_{pv}, V_{pv} and T denote the output current, the output voltage and the cell temperature of the PV module respectively; I_0 represents the diode's saturation current, and it is influenced by the temperature. We use the same data in [24]: $n = 1.5$ is the ideal PN junction characteristic factor, $K = 1.3805 \times 10^{-23}$ J/K, $q = 1.6 \times 10^{-19}$ C denote the Boltzmann's constant and the electronic charge respectively. I_{ph} represents the generated photocurrent, and it depends mainly on the radiation and cells temperature. I_{scr} and K_i denote the short-circuit current at a reference condition and the short-circuit temperature coefficient respectively. T_r and G are respectively the reference temperature and the solar irradiance (W/m^2). R_s is the series resistance of the cell and R_{sh} is the parallel resistance of the cell.

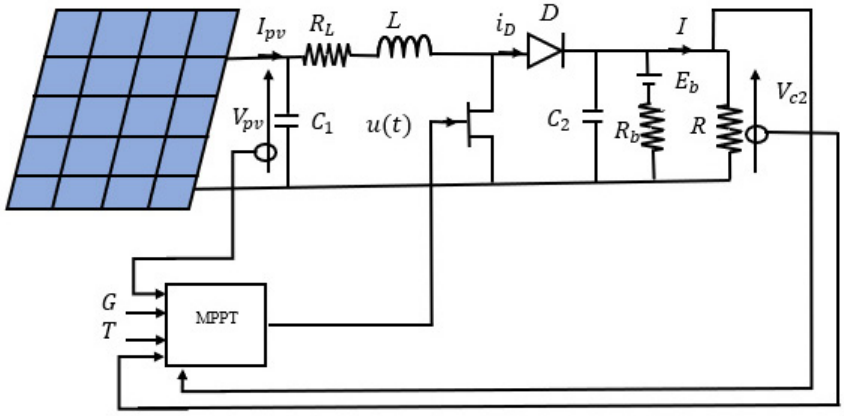

FIGURE 1. Global structure of the PV system with storage battery

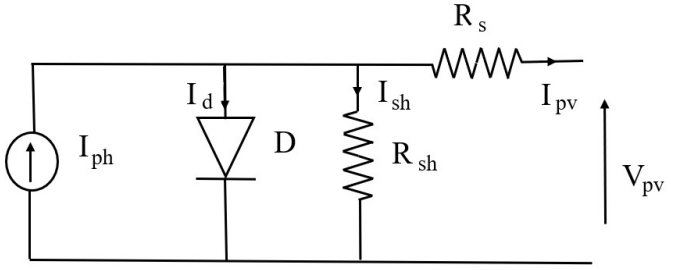

FIGURE 2. Equivalent circuit model of the PV cell

For a PV module composed of N_p strings in parallel, the mathematical model can be represented by the equation

$$I_{pv} = N_p I_{ph} - N_p I_0 \left[\exp\left(\frac{V_{pv} + R_s I_{pv}}{nV_T}\right) - 1\right] - N_p \left(\frac{V_{pv} + R_s I_{pv}}{N_s R_{sh}}\right) \tag{3}$$

where N_s is the number of cells in series per string.

Figure 3 shows P-V and I-V characteristics at different levels of solar irradiance G and temperatures T. It can be observed that the variation of the maximum power of PV panel, changes highly as a function of the solar irradiation and the cell temperature. From these curves, we can detect that the more temperature is low, the more cell generates power.

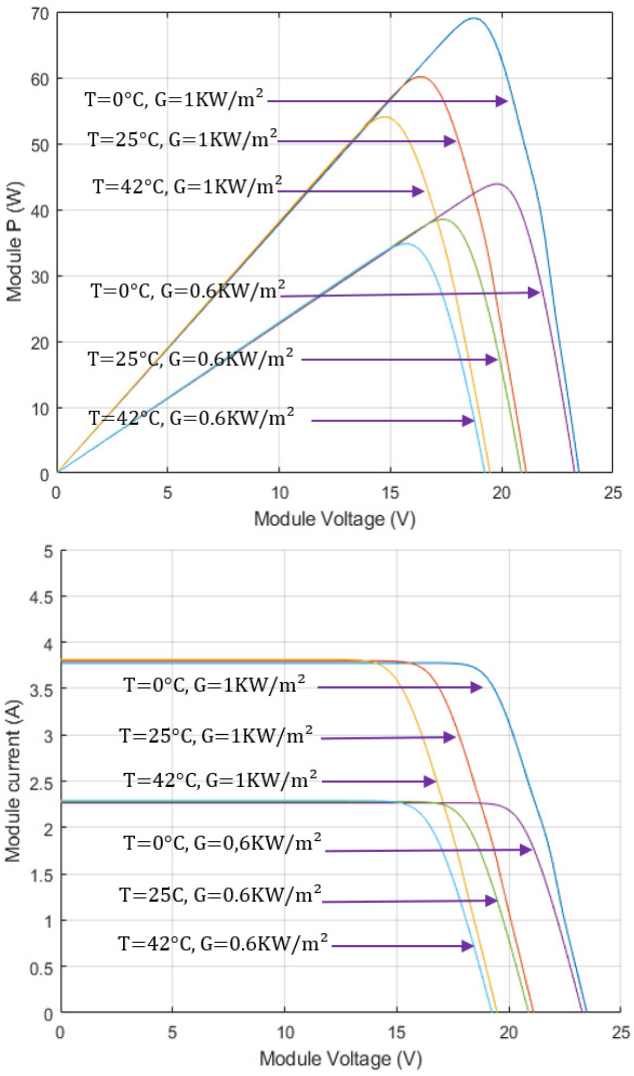

FIGURE 3. I-V and P-V characteristics of *MSX*60 PV in varying climatic conditions for a typical clear day

2.2. **DC-DC boost converter.** The DC-DC boost converter is shown in Figure 1. The dynamic model is described by two sets of linear differential equations according to the switch's states ON or OFF. In order to simplify the study, we will establish the MPPT command when the battery is fully charged. The differential equation of a DC-DC boost converter during the 'ON' state can be defined as [21]:

$$\begin{cases} \dfrac{dV_{pv}(t)}{dt} = -\dfrac{1}{C_1}(I_L(t) - I_{PV}(t)) \\ \dfrac{dI_L(t)}{dt} = \dfrac{1}{L}V_{pv}(t) - \dfrac{R_L}{L}I_L(t) \\ \dfrac{dV_{c2}(t)}{dt} = -\dfrac{1}{RC_2}V_{c2}(t) \end{cases} \tag{4}$$

and during the OFF period we have

$$\begin{cases} \dfrac{dV_{pv}(t)}{dt} = -\dfrac{1}{C_1}(I_L(t) - I_{PV}(t)) \\ \dfrac{dI_L(t)}{dt} = \dfrac{1}{L}V_{pv}(t) - \dfrac{R_L}{L}I_L(t) - \dfrac{1}{L}V_{c2}(t) \\ \dfrac{dV_{c2}(t)}{dt} = \dfrac{1}{C_2}I_L(t) - \dfrac{1}{RC_2}V_{c2}(t) \end{cases} \tag{5}$$

where V_{PV}, I_L and V_{c2} denote the output voltage, the inductor current and the input voltage, respectively.

The state space equation during the 'ON' period is defined as follows:

$$\dot{x}(t) = A_1 x(t) + E\omega(t) \tag{6}$$

And the state space equation during the 'OFF' period is given by the following equation

$$\dot{x}(t) = A_2 x(t) + E\omega(t) \tag{7}$$

where

$$A_1 = \begin{bmatrix} 0 & -\dfrac{1}{C_1} & 0 \\ \dfrac{1}{L} & -\dfrac{R_L}{L} & 0 \\ 0 & 0 & -\dfrac{1}{RC_2} \end{bmatrix}, \quad A_2 = \begin{bmatrix} 0 & -\dfrac{1}{C_1} & 0 \\ \dfrac{1}{L} & -\dfrac{R_L}{L} & -\dfrac{1}{L} \\ 0 & \dfrac{1}{C_2} & -\dfrac{1}{RC_2} \end{bmatrix}$$

$$E = \begin{bmatrix} \dfrac{1}{C_1} \\ 0 \\ 0 \end{bmatrix}, \quad x(t) = \begin{bmatrix} V_{pv}(t) \\ I_L(t) \\ V_{c2}(t) \end{bmatrix}, \quad \omega(t) = I_{pv}(t)$$

As a result, the dynamics of the PV conversion system can be rewritten in the following average model:

$$\dot{x}(t) = [A_1 x(t) + E\omega(t)]u(t) + [A_2 x(t) + E\omega(t)](1 - u(t)) \tag{8}$$

or equally,

$$\dot{x}(t) = A_2 x(t) + (A_1 - A_2)x(t)u(t) + E\omega(t) \tag{9}$$

as well,

$$\dot{x}(t) = A_2 x(t) + B(x(t))u(t) + E\omega(t) \tag{10}$$

with $u(t) \in [0, 1]$, where $B(x(t)) = \begin{bmatrix} 0 \\ \frac{V_{c2}(t)}{L} \\ -\frac{I_L(t)}{C_2} \end{bmatrix}$ and the duty ratio used as an input to control the power switch is denoted by $u(t)$.

2.3. **The perturb and observe (P&O) MPPT algorithm.** The simplicity of implementation of the P&O algorithm makes this technique the most widely used method in PV systems [27]. The principle of this method consists in disturbing the V_{PV} voltage of the GPV with a small amplitude around its initial value and analyzing the behavior of the resulting power variation P_{PV} [22] (show in Figure 4). If after a voltage disturbance, the PV power increases, the disturbance direction is maintained otherwise it is reversed to resume convergence towards the new MPP. The algorithm illustrating the P&O method is given in Figure 5.

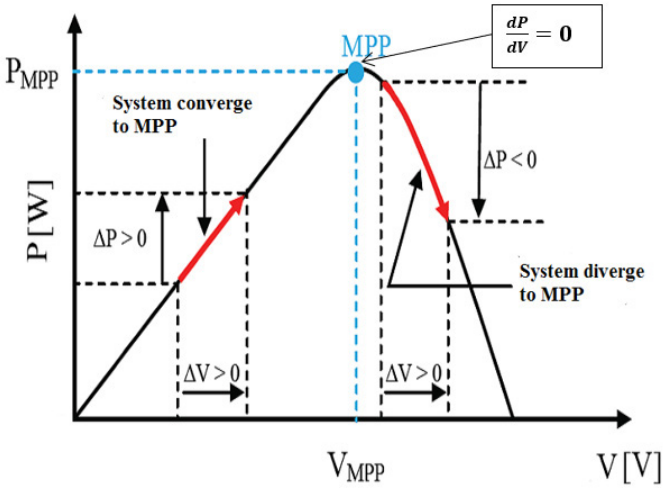

FIGURE 4. Operating principle of P&O method [22]

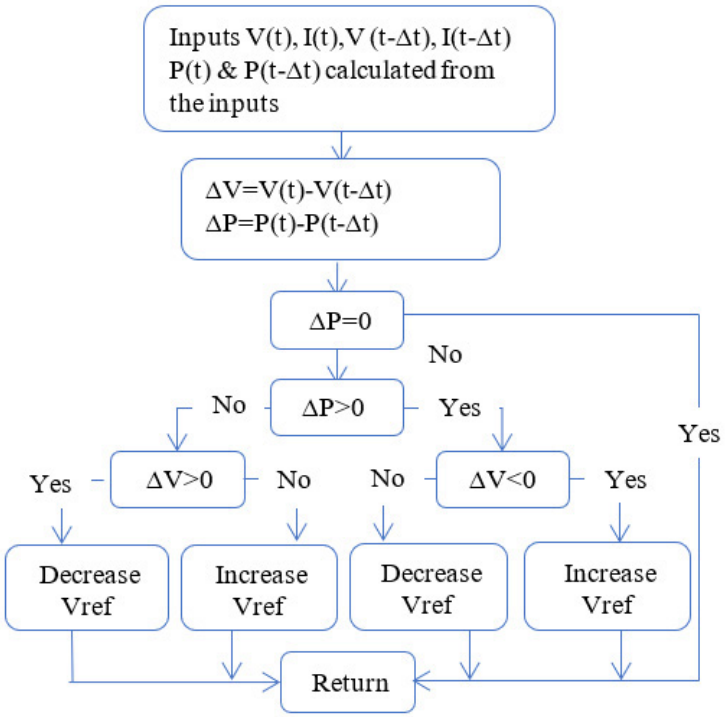

FIGURE 5. Maximum power point tracking algorithm (P&O)

Remark 2.1. *Despite the P&O algorithm is easy to implement, it has mainly the following problems.*

1) The PV system always operates in an oscillating mode.

2) The operation of the PV system may fail to track the maximum power point.

The general requirements of maximum power point tracking are low cost, simple implementation, and quick tracking under varying atmospheric conditions and minor power fluctuations. The main objective of the current work is to propose a T-S fuzzy controller for a PV system with battery storage with a guaranteed closed-loop stability region and reduce oscillations.

3. **T-S Fuzzy MPPT Control Design.** We will start with the boost converter's dynamic model, which will lead to the Takagi-Sugeno model, which we will use in the fuzzy control design stage.

3.1. **T-S fuzzy model for the boost converter.** The T-S fuzzy controller system follows the so-called fuzzy rules, which include IF-THEN statements, fuzzy sets, logic, and inference. These rules are extremely useful for depicting sophisticated controls and models and for connecting input and output variables of fuzzy controllers. Use the method based on T-S models proposed in [24], which are a very interesting mathematical representation of PV system, because they allow obtaining sufficient LMI conditions both for the stability analysis and controller gain design associated with each local model.

The T-S fuzzy functions for total membership are configured as follows:

$$\begin{cases} z_1(t) = V_{c2}(t) \\ z_2(t) = I_L(t) \end{cases} \tag{11}$$

The membership functions of the T-S fuzzy model are obtained by following the operations given in [24] as follows

$$\begin{aligned} F_{1,\min}(z(t)) &= \frac{z_1(t) - z_{1,\min}}{z_{1,\max} - z_{1,\min}} \\ F_{1,\max}(z(t)) &= 1 - F_{1,\min}(z(t)) \\ F_{2,\min}(z(t)) &= \frac{z_2(t) - z_{2,\min}}{z_{2,\max} - z_{2,\min}} \\ F_{2,\max}(z(t)) &= 1 - F_{2,\min}(z(t)) \end{aligned}$$

The expressions of the weighting functions h_i used are as follows

$$\begin{aligned} h_1(z(t)) &= F_{1,\min}(z(t))F_{2,\min}(z(t)) \\ h_2(z(t)) &= F_{1,\min}(z(t))F_{2,\max}(z(t)) \\ h_3(z(t)) &= F_{1,\max}(z(t))F_{2,\min}(z(t)) \\ h_4(z(t)) &= F_{1,\max}(z(t))F_{2,\max}(z(t)) \end{aligned}$$

The PV system is approximated by four fuzzy rules represented as follows:

Rule 1: If ($V_{c2}(t)$ is $F_{1,\min}$) and ($I_L(t)$ is $F_{2,\min}$) Then

$$\dot{x} = A_2 x(t) + B_1 u(t) + E\omega(t)$$

Rule 2: If ($V_{c2}(t)$ is $F_{1,\min}$) and ($I_L(t)$ is $F_{2,\max}$) Then

$$\dot{x} = A_2 x(t) + B_2 u(t) + E\omega(t)$$

Rule 3: If ($V_{c2}(t)$ is $F_{1,\max}$) and ($I_L(t)$ is $F_{2,\min}$) Then

$$\dot{x} = A_2 x(t) + B_3 u(t) + E\omega(t)$$

Rule 4: If ($V_{c2}(t)$ is $F_{1,\max}$) and ($I_L(t)$ is $F_{2,\max}$) Then

$$\dot{x} = A_2 x(t) + B_4 u(t) + E\omega(t)$$

$$B_1 = \begin{bmatrix} 0 \\ \dfrac{V_{c2\,\min}(t)}{L} \\ -\dfrac{I_{L\,\min}(t)}{C_2} \end{bmatrix}, \quad B_2 = \begin{bmatrix} 0 \\ \dfrac{V_{c2\,\min}(t)}{L} \\ -\dfrac{I_{L\,\max}(t)}{C_2} \end{bmatrix},$$

$$B_3 = \begin{bmatrix} 0 \\ \dfrac{V_{c2\max}(t)}{L} \\ -\dfrac{I_{L\min}(t)}{C_2} \end{bmatrix}, \quad B_4 = \begin{bmatrix} 0 \\ \dfrac{V_{c2\max}(t)}{L} \\ -\dfrac{I_{L\max}(t)}{C_2} \end{bmatrix}$$

The fuzzy rule-based system's overall output is given by

$$\dot{x}(t) = \sum_{i=1}^{4} h_i(z(t))(A_2 x(t) + B_i u(t) + E\omega(t)) \tag{12}$$

In order to facilitate the design of fuzzy controller, the following lemma is needed [23].

Lemma 3.1. [23] *For matrices T, Q, U, and W with appropriate dimensions and scalar ξ, the inequality*

$$T + W^T Q^T + QW < 0 \tag{13}$$

is fulfilled if the following condition holds:

$$\begin{bmatrix} T & * \\ \xi Q^T + UW & -\xi U - \xi U^T \end{bmatrix} < 0$$

3.2. **MPPT reference model.** The goal of this section is to develop a fuzzy controller that can follow a perfect reference model by driving the state of the PV system. The state equation of the MPPT reference model is defined as follows:

$$\dot{x}_r(t) = A_r x_r(t) + r(t) \tag{14}$$

where

$$A_r = \begin{bmatrix} 0 & -\dfrac{1}{C_1} & 0 \\ \dfrac{1}{L} & -\dfrac{R_L}{L} & -\dfrac{1}{L}(1-u_{opt}) \\ 0 & \dfrac{1}{C_2}(1-u_{opt}) & -\dfrac{1}{RC_2} \end{bmatrix}, \quad r(t) = \begin{bmatrix} \dfrac{I_{pvopt}}{C_1} \\ 0 \\ 0 \end{bmatrix}, \quad u_{opt} = \sqrt{\frac{V_{pvopt}}{RI_{pvopt}}}$$

As shown in the above representation, the reference model (14) is also nonlinear via the premise variable $z_r = (1 - u_{opt})$ and can be described by the following two rules:

Rule 1: If ($z_r(t)$ is $N_{\min}$) Then $\dot{x}_r(t) = A_{r1}x_r(t) + r(t)$

Rule 2: If ($z_r(t)$ is $N_{\max}$) Then $\dot{x}_r(t) = A_{r2}x_r(t) + r(t)$

The membership and weighting functions are defined as follows:

$$h_1(z_r(t)) = N_{\min}(z_r(t)) = \frac{z_r(t) - z_{r,\min}}{z_{r,\max} - z_{r,\min}}$$
$$h_2(z_r(t)) = N_{\max}(z_r(t)) = 1 - h_1(z_r(t))$$

The matrices of the reference model are defined as

$$A_{r1} = \begin{bmatrix} 0 & -\dfrac{1}{C_1} & 0 \\ \dfrac{1}{L} & -\dfrac{R_L}{L} & -\dfrac{1}{L}z_{r,\min} \\ 0 & \dfrac{1}{C_2}z_{r,\min} & -\dfrac{1}{RC_2} \end{bmatrix}, \quad A_{r2} = \begin{bmatrix} 0 & -\dfrac{1}{C_1} & 0 \\ \dfrac{1}{L} & -\dfrac{R_L}{L} & -\dfrac{1}{L}z_{r,\max} \\ 0 & \dfrac{1}{C_2}z_{r,\max} & -\dfrac{1}{RC_2} \end{bmatrix}$$

The global T-S fuzzy reference model can be summarized as follows:

$$\dot{x}_r(t) = \sum_{k=1}^{2} h_k(z_r(t))(A_{rk}x_r(t) + r(t)) \tag{15}$$

3.3. **Fuzzy controller design.** The main difference from the ordinary parallel distributed compensation controller is to add in the control law the term of the tracking error:

$$e(t) = x(t) - x_r(t)$$

Thus, to operate at the maximum power point, we must ensure that the tracking error converges to zero whatever the variations of insolation and temperature. As a result, the trajectory tracking problem is modeled as a fuzzy state feedback control system, with the following control law:

$$u(t) = \sum_{j=1}^{4} h_j(z(t))K_j(x(t) - x_r(t)) = \sum_{j=1}^{4} h_j(z(t))K_j e(t) \tag{16}$$

where K_j are linear feedback gain matrices to be developed.

The error dynamics of systems (12), (15), and (16) can be calculated as follows:

$$\begin{aligned}\dot{e}(t) = \sum_{i=1}^{4}\sum_{j=1}^{4}\sum_{k=1}^{2} h_i(z(t))h_j(z(t))h_k(z_r(t))[(A_2 + B_iK_j)e(t) \\ + (A_2 - A_{rk})x_r(t) + E\omega(t) - r(t)]\end{aligned} \tag{17}$$

Substituting the control law (16) in the fuzzy model (12) and using an augmented state-space form, the closed-loop system is given by

$$\dot{\bar{x}}(t) = \sum_{i=1}^{4}\sum_{j=1}^{4}\sum_{k=1}^{2} h_i(z(t))h_j(z(t))h_k(z_r(t)) \left[\bar{A}_{ijk}\bar{x}(t) + \bar{E}\bar{\omega}(t)\right] \tag{18}$$

where

$$\bar{x}(t) = \begin{bmatrix} e(t) \\ x_r(t) \end{bmatrix}, \quad \bar{\omega}(t) = \begin{bmatrix} \omega(t) \\ r(t) \end{bmatrix}, \quad \bar{E}(t) = \begin{bmatrix} E & -I \\ 0 & I \end{bmatrix},$$
$$\bar{A}_{ijk} = \begin{bmatrix} A_2 + B_iK_j & A_2 - A_{rk} \\ 0 & A_{rk} \end{bmatrix}$$

The disturbance due to the input voltage variation, including parameters (I_{pvopt} and I_{pv}), is denoted by $\omega(t)$, and $r(t)$ represents the external input which depends on climatic condition. The H_∞ performance can be formulated as follows to quickly attenuate the effect of disturbance on closed loop control system:

$$\int_0^\infty \bar{x}(t)\bar{Q}\bar{x}(t)dt \le \gamma^2 \int_0^\infty \bar{\omega}^T(t)\bar{\omega}(t)dt \tag{19}$$

where $\bar{Q} = \begin{bmatrix} Q_1 & 0 \\ 0 & 0 \end{bmatrix}$.

This study uses the H_∞ tracking method to make the PV system track its maximum power trajectory for different solar insolation and temperature levels, as well as guarantee a specified attenuation level against the external disturbance effect.

Now, we shall present sufficient conditions for the existence of a T-S fuzzy controller (16) that will force the PV generator to operate very close to the maximum power trajectory. The benefit of this approach is to reduce the maximum power tracking error even when climatic conditions change quickly. Based on the above analysis, we obtained the following theorem.

Theorem 3.1. *Given positive scalars α and ξ the closed-loop system* (18) *is asymptotically stable and the H_∞ performance* (19) *with the attenuation level γ is satisfied, if there are*

some matrices $P_1 > 0$, $P_2 > 0$, P_3, U, N_i, $i = 1, 2, 3, 4$ and a positive scalar γ solution for the following optimization problem:

$$\Psi_{iik} < 0, \quad k = 1, 2 \tag{20}$$

$$\Psi_{ijk} + \Psi_{jik} < 0, \quad k = 1, 2 \tag{21}$$

where

$$\Psi_{ijk} = \begin{bmatrix} \Psi_{ijk}^{11} & \Psi_{ijk}^{12} & P_1E & P_2 - P_1 & \Psi_{ijk}^{15} \\ * & \Psi_{ijk}^{22} & P_2E & P_3 - P_2 & \Psi_{ijk}^{25} \\ * & * & -\gamma^2 I & 0 & 0 \\ * & * & * & -\gamma^2 I & 0 \\ * & * & * & * & -\xi U - \xi U^T \end{bmatrix} \tag{22}$$

$$\begin{aligned} \Psi_{ijk}^{11} &= sym\{P_1A_2 + B_iN_j\} + Q_1 + \alpha P_1 \\ \Psi_{ijk}^{12} &= P_1(A_2 - A_{rk}) + P_2A_{rk} + \left(A_2^T P_2 + \lambda N_j^T B_i^T\right) + \alpha P_2 \\ \Psi_{ijk}^{15} &= \xi(P_1B_i - B_iU) + N_j^T \\ \Psi_{ijk}^{22} &= sym\{P_2(A_2 - A_{rk}) + P_3A_{rk}\} + \alpha P_3 \\ \Psi_{ijk}^{25} &= (\xi)(P_2B_i - \lambda B_iU) \end{aligned} \tag{23}$$

Furthermore, the controller gain matrices are given by $K_j = U^{-1}N_j$, $j = 1, 2, \ldots, r$.

Proof: Suppose that Inequalities (20) and (21) hold. The feasible solution of this inequality satisfies $-\xi U - \xi U^T < 0$, which implies that matrix U is nonsingular. Obviously, the LMI conditions (20) and (21) can be rewritten as follows:

$$\sum_{k=1}^{2} h_k \left[\sum_{i=1}^{4} h_i^2 \Psi_{iik} + \sum_{i=1}^{4-1} \sum_{j=i+1}^{4} h_i h_j (\Psi_{ijk} + \Psi_{jik}) \right] = \sum_{k=1}^{2} \sum_{i=1}^{4} \sum_{j=1}^{4} h_k h_i h_j \Psi_{ijk} < 0 \tag{24}$$

which is verified if

$$\Psi_{ijk} = \begin{bmatrix} T_{ijl} & * \\ \xi Q_i^T + UW_{jl} & -\xi U - \xi U^T \end{bmatrix} < 0 \tag{25}$$

with

$$\begin{aligned} T_{ijl} &= \begin{bmatrix} \Psi_{ijk}^{11} & \Psi_{ijk}^{12} & P_1E & P_2 - P_1 \\ * & \Psi_{ijk}^{22} & P_2E & P_3 - P_2 \\ * & * & -\gamma^2 I & 0 \\ * & * & * & -\gamma^2 I \end{bmatrix}, \\ Q_i &= \begin{bmatrix} P_1B_i - B_iU \\ (P_2B_i - \lambda B_iU) \\ 0 \\ 0 \end{bmatrix}, \quad W_{jl} = U^{-1} \begin{bmatrix} N_j & 0 & 0 & 0 \end{bmatrix} \end{aligned} \tag{26}$$

where Ψ_{ijk}^{11}, Ψ_{ijk}^{12} and Ψ_{ijk}^{22} are defined in (22).

Applying Lemma 3.1 obviously, the following condition holds

$$T_{ijl} + sym\left\{ \begin{bmatrix} P_1B_i - B_iU \\ (P_2B_i - \lambda B_iU) \\ 0 \\ 0 \end{bmatrix} U^{-1} \begin{bmatrix} N_j & 0 & 0 & 0 \end{bmatrix} \right\} < 0 \tag{27}$$

From (27), we have

$$T_{ijl} + \begin{bmatrix} \Upsilon_{i11} & \Upsilon_{ij12} & 0 & 0 \\ * & 0 & 0 & 0 \\ * & * & 0 & 0 \\ * & * & * & 0 \end{bmatrix} < 0 \tag{28}$$

where

$$\Upsilon_{i11} = sym\{(P_1 B_i - B_i U)U^{-1} N_j\}$$
$$\Upsilon_{ij12} = N_j^T U^{-T}(P_2 B_i - \lambda B_i U)^T$$

Substituting T_{ijl} in (26) into (28) and applying the change of variables $N_j = UK_j$ we obtain

$$\begin{bmatrix} \Phi_{ijk}^{11} & \Phi_{ijk}^{12} & P_1 E & P_2 - P_1 \\ * & \Psi_{ijk}^{22} & P_2 E & P_3 - P_2 \\ * & * & -\gamma^2 I & 0 \\ * & * & * & -\gamma^2 I \end{bmatrix} < 0 \tag{29}$$

$$\begin{aligned} \Phi_{ijk}^{11} &= sym\{P_1(A_2 + B_i K_j)\} + Q_1 + \alpha P_1 \\ \Phi_{ijk}^{12} &= P_1(A_2 - A_{rk}k) + P_2 A_{rk} + (A_2 + B_i K_j)^T P_2 + \alpha P_2 \end{aligned} \tag{30}$$

We note that $\bar{P} = \begin{bmatrix} P_1 & P_2 \\ P_2 & P_3 \end{bmatrix}$, the above inequality can be transformed to the next one:

$$\begin{bmatrix} sym\left\{\bar{P}\bar{A}_{ijk}\right\} + \bar{Q} + \alpha\bar{P} & \bar{P}\bar{E} \\ * & -\gamma^2 I \end{bmatrix} < 0 \tag{31}$$

Let us consider the Lyapunov function given by [26]

$$V(\bar{x}(t)) = \bar{x}(t)^T \bar{P}\bar{x}(t) \tag{32}$$

For the asymptotic stability with decay rate of the closed loop system, the condition is defined as follows

$$\dot{V}(\bar{x}(t)) < -\alpha V(\bar{x}(t)) \tag{33}$$

The derivative of (32) with respect to time satisfies

$$\begin{aligned} \dot{V}(\bar{x}(t)) = \sum_{k=1}^{2}\sum_{i=1}^{4}\sum_{j=1}^{4} h_k h_i h_j \left\{ \left[\bar{x}(t)^T \bar{A}_{ijk}^T + \bar{\omega}^T(t)\bar{E}^T\right] \bar{P}\bar{x}(t) \right. \\ \left. + \bar{x}(t)^T \bar{P}\left[\bar{A}_{ijk}\bar{x}(t) + \bar{E}\bar{\omega}(t)\right]\bar{x}(t) \right\} \end{aligned} \tag{34}$$

From (33) we have that

$$\dot{V}_1(\bar{x}(t)) = \dot{V}(\bar{x}(t)) + \alpha V(\bar{x}(t)) < 0 \tag{35}$$

Taking account of (34), if (31) holds, it can be easily verified that

$$\dot{V}_1(\bar{x}(t)) + \bar{x}(t)^T \bar{Q}\bar{x}(t) - \gamma^2 \bar{\omega}(t)^T \bar{\omega}(t) < 0 \tag{36}$$

Integrating both sides of Inequality (36) from 0 to ∞ yields

$$\begin{aligned} &\int_0^\infty \dot{V}_1 dt + \int_0^\infty \left(\bar{x}(t)^T \bar{Q}\bar{x}(t) - \gamma^2 \bar{\omega}(t)^T \bar{\omega}(t)\right) dt \\ &= V(\bar{x}(\infty)) - V(\bar{x}(0)) + \int_0^\infty \left(\bar{x}(t)^T \bar{Q}\bar{x}(t) - \gamma^2 \bar{\omega}(t)^T \bar{\omega}(t)\right) dt < 0 \end{aligned}$$

For zero initial condition, we obtain (19). This completes the proof. □

Remark 3.1. *It should be noted that in* [21, 24]*, the MPPT control for photovoltaic was studied using the LMI method, and a T-S reference model is constructed to provide the desired trajectory that must be tracked. In contrast to the previously stated LMI design methods, this paper uses the T-S fuzzy model based approach to present an MPPT control for photovoltaic systems with battery storage. The proposed method includes neither transformation matrices nor equality constraints, which simplifies the numerical solution. Moreover, the introduction of the scalar parameters* $\xi = \alpha = \lambda = 1$ *can ensure the feasibility of the results, but the selection of* α*,* λ *and* ξ *provides extra free dimensions in the solution space for the design condition.*

4. **Simulation Results.** We use numerical simulation in this section to demonstrate the efficiency and the benefits of the fuzzy controller approach applied to the boost DC-DC converter for the PV system with storage system, under variable climatic conditions, a comparison was made between the proposed T-S fuzzy controller and the traditional perturb and observe (P&O) algorithm. Here, we are using an *MSX*60 PV module, whose specifications are listed in Table 1. The parameters of the boost converter are chosen as [28], $C_1 = 100$ µF, $L = 3$ mH, $R_l = 0.001$ Ω, $R = 30$ Ω, $C_2 = 100$ µF. A lead-acid battery from the PowerSafe T-S series is used as the storage device. Table 2 shows the key characteristics of battery at temperature of (25°C). Figure 6 shows a diagram that illustrates the proposed fuzzy controller.

TABLE 1. *MSX*60 PV module

Parameters	Abbreviation	Value
Maximum power	P_{pvopt}	60 W
Maximum current	I_{pvopt}	3.5 A
Maximum voltage	V_{pvopt}	17.1 V
Short circuit current	I_{ph}	3.8 A
Open circuit voltage	V_{oc}	21.1 V

TABLE 2. Lead acid battery parameters

Parameters	Name	Value
C	Nominal capacity	200 Ah
R_{Bat}	Internal resistor	0.64×12 (7.68 mΩ)
E_{Bat}	Nominal voltage	2×12 V (24 V)

By solving the LMIs condition in Theorem 3.1, we get the minimum H_∞ disturbance attenuation level $\gamma_{\min} = 0.3$, and the following controller gains.

$$K_1 = [0.0012 \quad -0.0462 \quad -0.1088], \quad K_2 = [-0.0000 \quad 0.0611 \quad -0.0034]$$
$$K_3 = [0.0002 \quad 0.0008 \quad -0.0229], \quad K_4 = [0.0002 \quad 0.0106 \quad -0.0506]$$

In order to verify the validity of the designed control scheme, real profile measurements temperature and solar irradiance were used. Figure 7 depicts an example of real daily climate data from the National Institute of Meteorology for the region of Oujda, Morocco.

The first simulation focuses on controlling the boost DC-DC converter in the event of weather changes, using the proposed MPPT method. The comparison results between P&O and our method are depicted in Figures 8-10.

These figures, in particular, show the responses of the PV current, PV voltage, and PV power to varying solar irradiation and temperatures. The T-S fuzzy controller, as

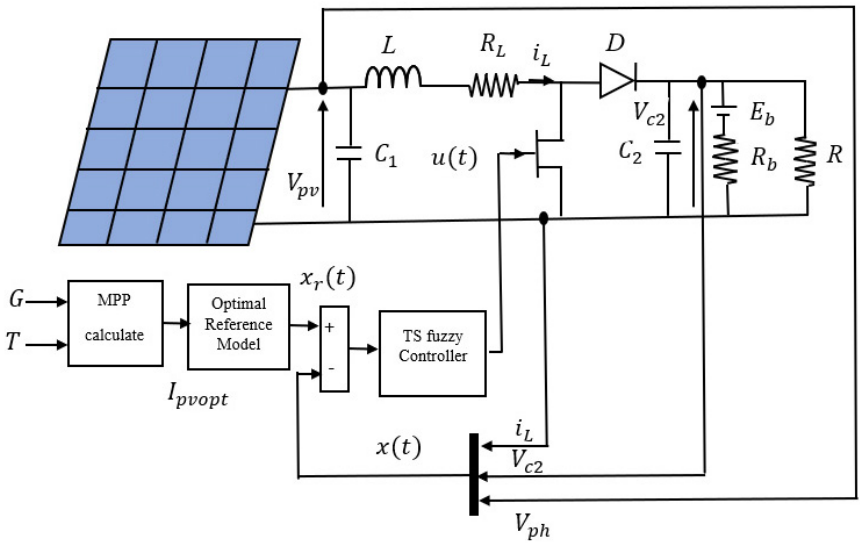

FIGURE 6. MPPT fuzzy structure of PV system

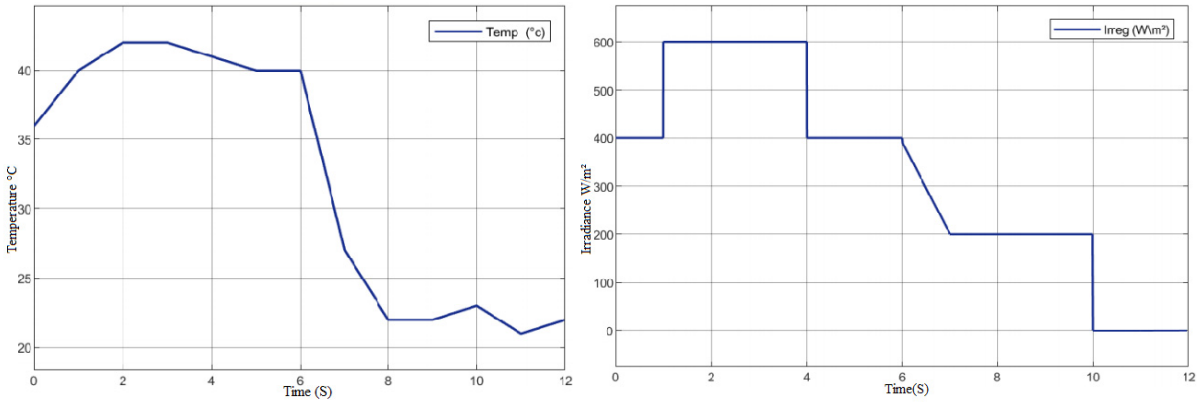

(a) (b)

FIGURE 7. Varying level of weather conditions: (a) temperature profile; (b) solar irradiance profile

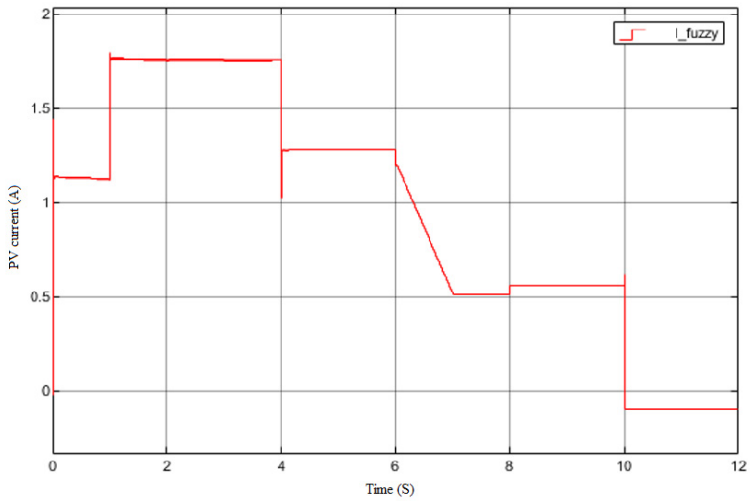

FIGURE 8. PV current curves comparison under various atmosphere

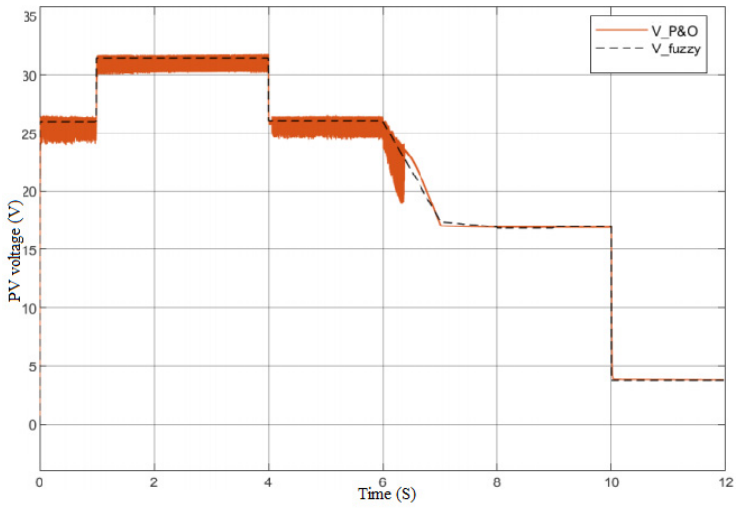

FIGURE 9. PV voltage curves comparison under various atmosphere

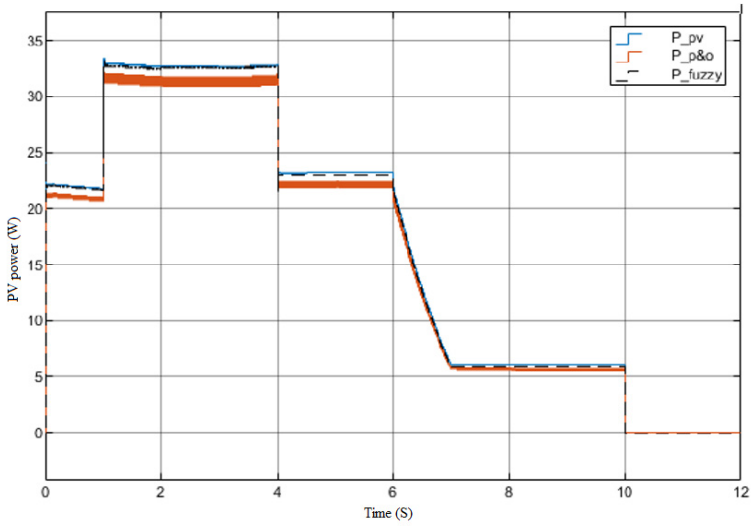

FIGURE 10. PV power curves comparison under various atmosphere

previously mentioned, has a fast dynamic response without oscillation. By examining Figures 8-10, it is clear that the proposed solution effectively generates the MPP tracking. For instance, the maximum irradiance and temperature levels during the interval time $t = [2, 6]$ s are $G = 600$ W/m^2 and $T = 42°$C, respectively. The optimum current and voltage of the PV module in this condition are about 1.81 A and 18.3 V, respectively. The maximum power of the PMPP PV module under the same irradiance and temperature conditions is PMPP = 35 W (Figure 3). We confirm that the proposed control successfully tracks the maximum power of the PV system with a relative uncertainty of 5.36% which corresponds to an efficiency of 94.63%.

By comparing the P&O algorithms, it is shown that the system's performance under the proposed approach yields a good dynamic performance characterized by a smoother curve, faster response, and the best tracking of the reference trajectory.

This simulation also allowed us to see the behavior of the battery associated with the PV system controlled by the fuzzy T-S controller. The SOC profile for one cycle is shown in Figure 11, where I_b denotes the battery current and V_b denotes the voltage, with $I_b < 0$ during charging and $I_b > 0$ during discharge.

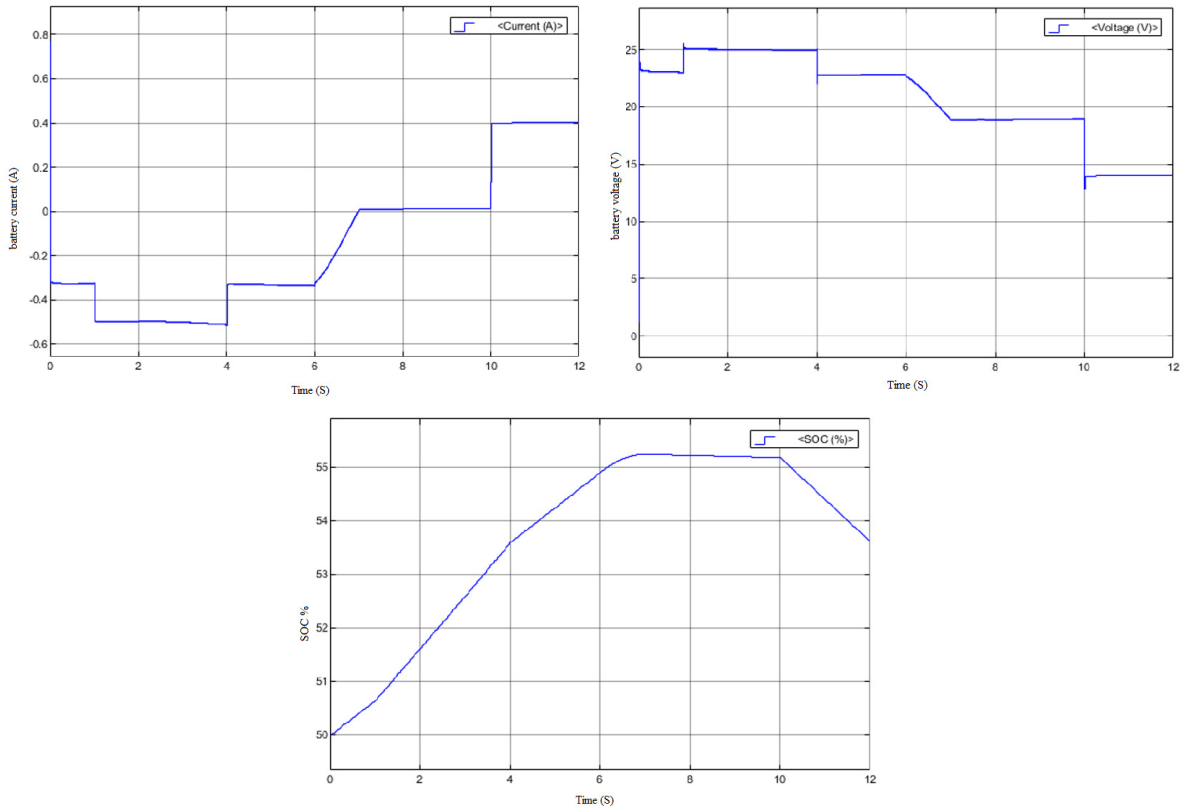

FIGURE 11. Evolution of battery current, battery voltage

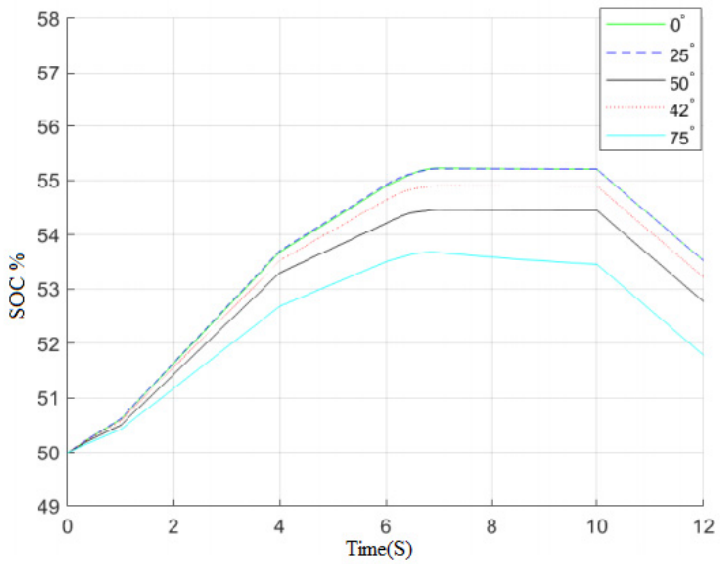

FIGURE 12. The battery charge curve using different temperature values

The second simulation aims to show the influence of ambient temperature on the state of charge and discharge of the battery. The battery storage voltage (V_b) and current (I_b) under the change of solar irradiance are shown in Figure 12 for different temperatures. We notice that the SOC of the battery varies considerably with temperature. At high temperatures, the SOC increases more slowly which corresponds to a slower charge. The influence of temperature appears during battery charging, but during discharge the curves

are parallel, indicating that the battery is discharging at the same rate regardless of the ambient temperature.

The obtained simulation results demonstrate that the TS fuzzy method outperforms the P&O algorithms in terms of tracking performance. The provided control method can ensure closed-loop system stability and its gains are parameterized in terms of a linear matrix inequality problem that can be solved efficiently.

5. **Conclusions.** The MPPT technique for a PV conversion method for a class of T-S fuzzy continuous-time method was studied in this paper. Using the Lyapunov function, appropriate conditions are extracted for the existence of a fuzzy controller. The design conditions are in linear matrix inequalities (LMIs) format. Our methodology helps us to minimize tracking time even while considering changing climatic conditions, which is an advantage over other literature approaches. It should be pointed out that the introduction of the slack variables provides more flexibility but the computational complexity increases. This result will be extended to fuzzy observer-based control using a buck converter.

REFERENCES

[1] R. Perez (edt.), Solor resource voriobility, in *Wind Field and Solar Radiation Characterization and Forecasting: A Numerical Approach for Complex Terrain*, vol.28, pp.149-170, 2018.

[2] T. Tameghe and T. Andy, Modeling and simulation of a wind-diesel twinning system supplying a local load, *ProQuest Dissertations and Theses*, University of Quebec in Abitibi-Temiscamingue, vol.26, pp.1-249, 2012.

[3] W.-T. Huang, K.-C. Yao, H.-C. Luo, H.-T. Chen, Y.-R. Chang, Y.-D. Lee and Y.-H. Ho, Prediction of photovoltaic power output for microgrids using back-propagation neural network, *ICIC Express Letters, Part B: Applications*, vol.10, no.3, pp.211-218, 2019.

[4] T. T. H. Pham, C. Clastres, F. Wurtz, S. Bacha and S. Ploix, Implementation of optimization for the sizing and feasibility studies of multi-source electrical systems in the building IBPSA France, *www.ibpsafrance.net*, pp.1-13, 2008.

[5] M. Mosa, M. B. Shadmand, R. S. Balog et al., Efficient maximum power point tracking using model predictive control for photovoltaic systems under dynamic weather condition, *IET Renew. Power Gener.*, vol.11, no.11, pp.1401-1409, 2017.

[6] N. Ali, H. Armghan, I. Ahmad, A. Armghan, S. Khan and M. Arsalan, Backstepping based non-linear control for maximum power point tracking in photovoltaic system, *Sol. Energy*, vol.159, pp.134-141, 2018.

[7] Y. Chaibi, *Modeling and Optimization of a Standalone Photovoltaic System Supplying an Alternative Load*, Ph.D. Thesis, National School of Arts and Crafts, Moulay Ismail University, Meknes, pp.1-132, 2019.

[8] R. Alik and A. Jusoh, Modified perturb and observe (P&O) with checking algorithm under various solar irradiation, *Sol. Energy*, vol.148, pp.128-139, 2017.

[9] H. Bounechba, A. Bouzid, H. Snani and A. Lashab, Real time simulation of MPPT algorithms for PV energy system, *Int. J. Electr. Power Energy Syst.*, vol.83, pp.67-78, 2016.

[10] S. K. Kollimalla and M. K. Mishra, Variable perturbation size adaptive P&O MPPT algorithm for sudden changes in irradiance, *IEEE Trans. Sustain. Energy*, vol.5, pp.718-728, 2014.

[11] Y. Hong, S. N. Pham, T. Yoo, K. Chae, K. H. Baek and Y. S. Kim, Efficient maximum power point tracking for a distributed PV system under rapidly changing environmental conditions, *IEEE Trans. Power Electron.*, vol.30, pp.4209-4218, 2015.

[12] A. Al Nabulsi and R. Dhaouadi, Efficiency optimization of a DSP-based standalone PV system using fuzzy logic and dual-MPPT control, *IEEE Trans. Industrial Informatics*, vol.8, pp.573-584, 2012.

[13] R. Chaibi, I. E. Rachid, E. H. Tissir and A. Hmamed, Finite frequency static output feedback H_∞ control of continuous-time T-S fuzzy systems, *Journal of Circuits, Systems, and Computers*, vol.28, no.2, 2018.

[14] T. Takagi and M. Sugeno, Fuzzy identification of systems and its application to modeling and control, *IEEE Trans. Syst. Man and Cybernetics*, vol.15, pp.116-132, 1985.

[15] R. Chaibi, H. E. Aiss, A. E. Hajjaji and A. Hmamed, Stability analysis and robust H_∞ controller synthesis with derivatives of membership functions for T-S fuzzy systems with time-varying delay:

Input-output stability approach, *International Journal of Control, Automation and Systems*, vol.18, pp.1-13, 2020.
[16] R. Chaibi, E. H. Tissir, A. Hmamed, E. M. E. Adel and M. Ouladsine, Static output feedback controller for continuous-time fuzzy systems, *International Journal of Innovative Computing, Information and Control*, vol.15, no.4, pp.1469-1484, 2019.
[17] B. S. Chen and S. J. Ho, Multiobjective tracking control design of TS fuzzy systems: Fuzzy Pareto optimal approach, *Fuzzy Sets and Systems*, vol.290, pp.39-55, 2016.
[18] C. S. Chiu and Y. L. Ouyang, Robust maximum power tracking control of uncertain photovoltaic systems: A unifield T-S fuzzy model-model based approach, *IEEE Trans. Control Systems Technology*, vol.19, no.6, pp.1516-1526, 2011.
[19] A. R. Reisi, M. H. Moradi and H. Showkati, Combined photovoltaic and unified power quality controller to improve power quality, *Sol. Energy*, vol.88, pp.154-162, 2013.
[20] J. Zhao, X. Zhou, Y. Ma and W. Liu, A novel maximum power point tracking strategy based on optimal voltage control for photovoltaic systems under variable environmental conditions, *Sol. Energy*, vol.122, pp.640-649, 2015.
[21] M. Allouche, K. Dahech and M. Chaabane, Multiobjective maximum power tracking control of photovoltaic systems: T-S fuzzy model-based approach, *Soft Comput.*, vol.22, pp.2121-2132, DOI: 10.1007/s00500-017-2691-7, 2018.
[22] C. Cedric, *Energy Optimization of the Electronic Adaptation Stage Dedicated to Photovoltaic Conversion*, Thesis, University of Toulouse III, 2008.
[23] X. H. Chang, L. Zhang and J. H. Park, Robust static output feedback H_∞ control for uncertain fuzzy systems, *Fuzzy Sets and Systems*, vol.273, pp.87-104, 2015.
[24] M. Allouche, K. Dahech, M. Chaabane and D. Mehdi, Fuzzy observer-based control for maximum power-point tracking of a photovoltaic system, *International Journal of Systems Science*, vol.49, no.5, pp.1061-1073, 2018.
[25] H. Zhang, R. Wang, J. Wang and Y. Shi, Robust finite frequency H_∞ static-output-feedback control with application to vibration active control of structural systems, *Mechatronics*, vol.24, no.4, pp.354-366, 2014.
[26] C. H. Fang, Y. S. Liu, S. W. Kau, L. Hong and C. H. Lee, A new LMI-based approach to relaxed quadratic stabilization of TS fuzzy control systems, *IEEE Trans. Fuzzy Systems*, vol.14, no.3, pp.386-397, 2006.
[27] M. Rezkallah, A. Hamadi, A. Chandra, B. Singh and A. Hamadi, Design and implementation of active power control with improved P&O method for wind-PV-battery-based standalone generation system, *IEEE Trans. Ind. Electron.*, vol.65, pp.5590-5600, 2018.
[28] S. Motahhir, A. E. Ghzizal, S. Sebti and A. Derouich, MIL and SIL and PIL tests for MPPT algorithm, *Cogent Engineering*, vol.4, no.1, 2017.

Author Biography

Karima El Hammoumi received the State Engineer diploma in Automatic Control and Industrial Computing in 1985 and the DESA in 'Industrial Process Control' in 2001 from the École Mohammadia d'Ingénieurs, Rabat, Morocco. She obtained the Doctorate degree in Renewable Energies from the University Sidi Mohamed Ben Abdellah Fez, Morocco in July 2021. Professor El Hammoumi is currently a professor at the École Supérieure de Technologie, Université Sidi Mohamed Ben Abdellah, Fès, Morocco. Her research interests automatic control systems, renewable energy, smart grid and battery storage.

Redouane Chaibi received the Master in Signals Systems and Computing from University of Sidi Mohammed Ben Abdellah, Faculty of Sciences, Fez, Morocco in 2014. He obtained the Doctorate degree in automatic control from Sidi Mohamed Ben Abdellah University (Fès, Morocco, 2019), Department of Physics. His research interests include robust control, fuzzy systems, LMIs, sum of squares, and renewable energy.

Rachid El Bachtiri was born in Midelt, Morocco in November 1964. He received the Electrical Engineering diploma from the École Mohammadia d'Ingénieurs, Rabat, Morocco in July 1988, and the Doctorate on applied sciences from the Université Catholique de Louvain, Louvain-la-Neuve, Belgium in January 1997.

He is a professor at the École Supérieure de Technologie, Université Sidi Mohamed Ben Abdellah, Fès, Morocco. Responsible of a group of scientific researchers "équipe de recherche en électrotechnique, électronique de puissance et énergies renouvelables". His research interests are motor drives, power electronic converters, automatic control systems and renewable energy.

Prof. El Bachtiri is currently head of the Department of Electrical and Computer Engineering, and expert at the national scientific and technical research center, Rabat, Morocco.